




## ARTICLE OPEN



# Disruption of macroscale functional network organisation in patients with frontotemporal dementia

A. Bouzigues<sup>1,2</sup>, V. Godefroy<sup>3</sup>, V. Le Du<sup>1</sup>, L. L. Russell<sup>2</sup>, M. Houot<sup>1,4</sup>, I. Le Ber<sup>1,4</sup>, B. Batrancourt<sup>1</sup>, R. Levy<sup>1,4</sup>, J. D. Warren<sup>2</sup>, J. D. Rohrer<sup>2</sup>, D. S. Margulies<sup>5,6</sup> and R. Migliaccio<sup>1,4</sup>

© The Author(s) 2024

Neurodegenerative dementias have a profound impact on higher-order cognitive and behavioural functions. Investigating macroscale functional networks through cortical gradients provides valuable insights into the neurodegenerative dementia process and overall brain function. This approach allows for the exploration of unimodal-multimodal differentiation and the intricate interplay between functional brain networks. We applied cortical gradients mapping to resting-state functional MRI data of patients with frontotemporal dementia (FTD) (behavioural-bvFTD, non-fluent and semantic) and healthy controls. In healthy controls, the principal gradient maximally distinguished sensorimotor from default-mode network (DMN) and the secondary gradient visual from salience network (SN). In all FTD variants, the principal gradient's unimodal-multimodal differentiation was disrupted. The secondary gradient, however, showed widespread disruptions impacting the interactions among all networks specifically in bvFTD, while semantic and non-fluent variants exhibited more focal alterations in limbic and sensorimotor networks. Additionally, the visual network showed responsive and/or compensatory changes in all patients. Importantly, these disruptions extended beyond atrophy distribution and related to symptomatology in patients with bvFTD. In conclusion, optimal brain function requires networks to operate in a segregated yet collaborative manner. In FTD, our findings indicate a collapse and loss of differentiation between networks not solely explained by atrophy. These specific cortical gradients' fingerprints could serve as a functional signature for identifying early changes in neurodegenerative diseases or potential compensatory processes.

*Molecular Psychiatry*; <https://doi.org/10.1038/s41380-024-02847-4>

## INTRODUCTION


Complex behaviours and higher-order cognition rely on distributed brain systems working synergistically for both serial and parallel processing [1, 2]. Extensively studied over the past 30 years, these functional networks are investigated by measuring temporal correlations between distributed and adjacent brain areas at rest [3]. Some networks, like visual or sensorimotor networks, are implicated in sensory processing, while others, such as the salience network (SN) and the default-mode network (DMN), are crucial for higher-order cognitive tasks like detecting salient stimuli or mind wandering. Examining functional networks through resting-state functional magnetic resonance imaging (rs-fMRI) to measure functional connectivity (FC) between regions [3, 4] is thus valuable to understand how neurodegeneration affects the brain and consequently, cognitive and behavioural functions.

Pioneering studies in resting-state FC have suggested that brain networks show both inter-network correlations and anticorrelations, meaning that cognitive and behavioural functions are not simply due to the activation of certain networks but also to an

interplay between networks involving the simultaneous decrease and increase of activity within different networks [5]. These activities play a crucial role in the brain's functional architecture, emerging during brain development [5, 6]. Similarly, changes in FC during aging and neurodegeneration involve not only abnormalities within networks but also a change of the interactions between large-scale networks [7, 8].

With this in mind, cortical gradient mapping offers a lens through which to characterise the relationship between connectivity patterns of macroscale functional networks in low-dimensional space. Applied to a large group of healthy individuals, this method describes a principal gradient of connectivity differentiation along the cortical surface, with sensory cortices presenting maximal FC pattern differences from regions involved in transmodal association processing (Fig. 1) [9]. In psychiatric and neurological disorders, gradient mapping identifies a *dedifferentiation* between sensory and transmodal networks such as ischaemic stroke [10], autism spectrum disorders [11], generalised epilepsy [12], depression [13, 14] and schizophrenia [15]. In such clinical conditions, the FC space in which the networks operate in

<sup>1</sup>Paris Brain Institute – Institut du Cerveau (ICM), Sorbonne Université, Inserm U1127, CNRS UMR 7225, AP-HP - Hôpital Pitié-Salpêtrière, Paris, France. <sup>2</sup>Dementia Research Centre, Queen Square Institute of Neurology, University College London, London, United Kingdom. <sup>3</sup>Centre de Recherche en Neurosciences de Lyon (CRNL), Université Claude Bernard Lyon 1, Inserm U1028, CNRS UMR 5292, F-69500 Bron, France. <sup>4</sup>Department of Neurology, Institute of Memory and Alzheimer's Disease, Centre of Excellence of Neurodegenerative Disease, Hôpital Pitié-Salpêtrière, Paris, France. <sup>5</sup>Integrative Neuroscience and Cognition Center, Université de Paris Cité, CNRS, Paris, France. <sup>6</sup>Wellcome Centre for Integrative Neuroimaging, FMRIB, Nuffield Department of Clinical Neurosciences, University of Oxford, Oxford, United Kingdom.

email: arabella.bouzigues@icm-institute.org; lara.migliaccio@gmail.com

Received: 24 January 2024 Revised: 8 November 2024 Accepted: 13 November 2024

Published online: 24 November 2024

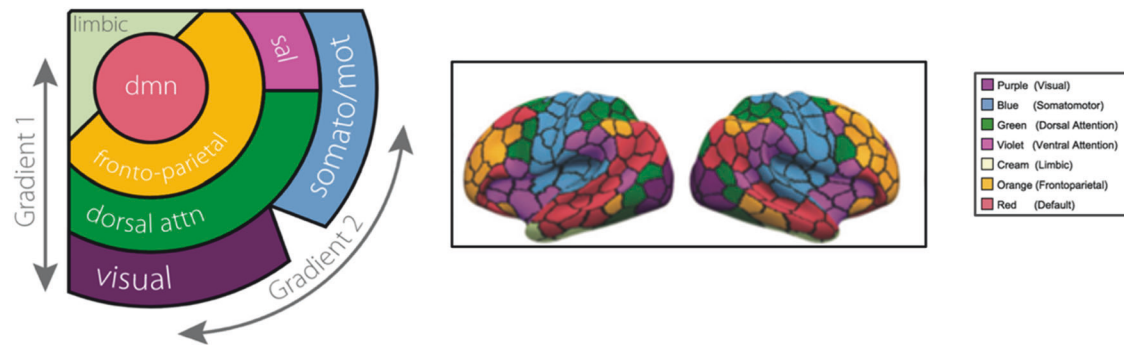


**Fig. 1 Schematic representation of spatial relationships of canonical resting-state networks and corresponding brain areas.** Cortical connectivity gradients reflecting processing hierarchies spanning sensory and transmodal areas and the seven resting-state network parcellation on the cortical surface, colour coded according to previous work (Yeo et al. [31], adapted from Margulies et al. [9].

contracts and networks become *dedifferentiated*. *Dedifferentiation* means that the neural representations of perceptual and conceptual information are less distinctive [16]. Thus, networks will have more similar patterns of connectivity and their activity may be less specific. This points towards an alteration of the interplay between networks, whereby there is a smaller difference between the activity elicited by a brain region's preferred and less preferred stimuli. Gradient mapping presents advantages over other methods by minimising prior, not assuming sharp boundaries between functional networks, and therefore enabling the investigation of the interrelationships between functional networks within a continuous FC space. It has been suggested that low-dimensional gradients provide a realistic model of brain functioning and could better predict behaviour and cognition than conventional edge-based analyses [17].

Frontotemporal dementia (FTD) is a heterogeneous group of neurodegenerative conditions presenting with distinct deterioration of behaviour, language and/or motor functions involving frontotemporal brain regions. Patients with behavioural-variant of FTD (bvFTD) show behavioural changes including apathy, disinhibition and impaired social cognition [18]. These patients show grey matter atrophy within anterior frontal, temporal, cingulate and insula cortices. In the language variants of primary progressive aphasia (PPA), patients with nonfluent variant (nfvPPA) present with speech apraxia and agrammatism while patients with semantic variant (svPPA) show anomia and impaired word comprehension [19]. While patients with nfvPPA show atrophy throughout the frontotemporal regions, particularly the motor and supplementary motor cortices, patients with svPPA have focal anterior temporal lobe damage. FTD has been proposed as a 'molecular nexopathy', where a specific conjunction of pathogenetic protein and neural circuit characteristics leads to the disease's manifestation [20]. Nexopathies target particular types of network connections, transcending canonical macro-network boundaries. There is a growing body of evidence on FC changes across this FTD spectrum [21–23]. However, reported findings remain variable and their contribution to better understanding brain dynamics, effects of neurodegeneration and clinical consequences is debated.

The aim of the present study was to apply cortical gradient mapping to investigate FC changes in patients affected by bvFTD, svPPA and nfvPPA. We aimed to find a principal gradient of macroscale functional network organisation, spanning from the DMN to primary sensory networks in controls and anticipated that this would be broadly maintained in the FTD patient groups. However, our first hypothesis was that all patients would show evidence of an overall constriction of FC space compared with controls (i.e. sensory and transmodal networks would be *dedifferentiated*). Secondly, in view of the clinical symptoms and associated patterns of atrophy, we expected that patients with

bvFTD would show the most widespread alterations of macroscale functional network organisation. Finally, we expected such network changes to be functionally relevant and relate to these patients' clinical symptoms.

## METHODS

### Subjects

Participants were recruited through two independent research studies within two research centres. Data collection from site 1 was part of the ECOCAPTURE study, sponsored by the French national institute for biomedical research (INSERM, C16-87), based at the Paris Brain Institute (more details here: <https://www.clinicaltrials.gov/ct2/show/NCT03272230>). Data collection from site 2 was part of the Longitudinal Investigation of FTD (LIFTD) study which took place at the Dementia Research Centre within University College London (more details here: <https://www.ucl.ac.uk/drc/research/frontotemporal-dementia>). A total of 129 participants were included in this study; 52 healthy control subjects and 42 patients with bvFTD across both sites, as well as 17 patients with svPPA and 18 with nfvPPA from site 2 (Table 1). Diagnoses were established based on current internationally recognised diagnostic criteria [18, 19]. Five patients with bvFTD from site 1 and one patient with bvFTD from site 2 had a pathological expansion in the C9 open reading frame 72 gene, four patients with nfvPPA were carriers of a progranulin C31fs mutation. There were no significant differences in age, education level, gender and MMSE scores between the two sites for each participant group ( $p > 0.05$ ), thus these independently acquired datasets were merged for subsequent analyses.

### Cognitive assessments

Participants carried out extensive clinical, cognitive and behavioural assessments as described previously in these datasets [24, 25]. Tests in common to both sites and used for the purpose of this study included the Mini Mental State Examination (MMSE), to assess global cognitive status and disease severity, and the mini-Social cognition & Emotional Assessment battery [26] to evaluate deficits in social cognition (miniSEA). Socioemotional deficits due to impaired social cognition are a hallmark of bvFTD clinical phenotype. Mean scores, standard deviations and sample sizes are presented in Table 1. Patient groups' and controls' performance on these cognitive tests were compared using *t*-tests.

### Imaging data acquisition and preprocessing

Volumetric T1 scans and resting-state fMRI scans were acquired at the neuroimaging core facility (CENIR) of the Paris Brain Institute and at University College London Hospital (UCLH). Sites were respectively equipped with a 3T Siemens Prisma and Trio whole-body scanner and a 12-channel head coil. T1-weighted images were acquired using a magnetisation prepared rapid acquisition gradient echo pulse sequence (MPRAGE). Site 1 anatomical protocol involved TR = 2.4 s TE = 2.17 ms; TE = 2.17 ms; flip angle = 8°; voxel size = 1 mm isotropic; slice thickness = 0.7 mm. Site 2 anatomical protocol involved TR = 2.4 s TE = 2 s; TE = 2.93 ms; flip angle = 8°; voxel size = 1 mm isotropic; slice thickness = 1.1 mm. Functional data based on the blood oxygenation level-dependent (BOLD) signal were acquired using a T2\*-weighted echo-planar image (EPI) pulse

**Table 1.** Demographic details for controls and each FTD patient group.

Group	N	Site (1:2)	Age	Sex (F:M)	Education	MMSE	Disease Duration	Mutation	miniSEA
Controls	52	18:34	63.6 ± 6.4	27:25	14.9 ± 3.0	29.4 ± 0.8	-	-	26.0 ± 1.48 (N = 28)
bvFTD	42	22:20	65.9 ± 7.7	12:30	14.2 ± 3.9	23.2 ± 4.0	4.2 ± 2.1	5 (C9orf72)	19.2 ± 4.99 (N = 23)
svPPA	17	0:17	64.0 ± 6.7	5:12	14.9 ± 3.0	22.8 ± 7.9	4.5 ± 1.7	-	-
nvPPA	18	0:17	70.6 ± 8.5	9:9	13.5 ± 2.6	20.9 ± 9.3	3.6 ± 1.5	4 (GRN C31fs)	-

Age and Disease Duration are presented as mean number of years ± standard deviation, MMSE and miniSEA are presented as mean score ± standard deviation, with additional sample size included for miniSEA. Site is presented as number of participants recruited from site 1 to site 2 ratio and sex as number of females to males ratio. Mutation is presented as number of mutation carriers and associated mutation. bvFTD behavioural variant of FTD, svPPA semantic variant of primary progressive aphasia, nvPPA non-fluent variant of primary progressive aphasia, MMSE Mini Mental State Examination, C9orf72 expansion repeat in the C9 open reading frame 72 gene, GRN programulin, miniSEA mini Social Emotional Assessment.

sequence. Site 1 functional protocol involved TR = 2050 ms, TE = 25 ms, flip angle = 80°, oblique axial slices of the brain were acquired at 290 or 436 time points with a voxel resolution of 2 mm (with two types of acquisition of different timeseries lengths). Site 2 functional protocol involved TR = 2500 ms, TE = 30 ms, flip angle = 80°, oblique axial slices of the brain were acquired at 200 time points with a voxel resolution of 2 mm. Participants were asked to lie with their eyes closed, without falling asleep during the resting-state acquisition run.

T1 scans and fMRI resting-state time series for all participants were preprocessed using fMRIPrep 21.0.1 [27], an automated Nipype-based preprocessing pipeline for fMRI data implemented in Python, which uses tools from software packages including FSL, ANTs, FreeSurfer and AFNI. Briefly, the pipeline included bias field correction, skull stripping, brain tissue segmentation, slice time correction, correction for head motion parameters, co-registration to corresponding structural image, and non-linear spatial normalisation to MNI space. Further details on anatomical and functional data preprocessing can be found in Supplementary Methods.

### Imaging data analysis

**Anatomical scans.** Measures of cortical thickness were obtained using FreeSurfer's automated anatomical statistics extraction pipeline for each participant and for each parcel of the Schaefer atlas (400 parcels). To transfer the Schaefer parcellation volume to subject space, we used the Multi Atlas Transfer Tool [28]. To show structural grey matter differences in patient groups compared to controls, we averaged cortical thickness for each parcel within each patient group and presented these as percentage cortical thickness of control mean.

**Resting-state scans.** We used mean framewise-displacement [29] as a quality assurance parameter for each subject's resting-state timeseries. Thus, subjects were included in subsequent analyses if their mean framewise head displacement in the MRI was below the threshold of 0.55 mm, as used in previous work with similar patient populations. Six patients with bvFTD (three from each site) and two with svPPA did not meet these criteria and were therefore excluded from subsequent analyses.

To remove physiological and other sources of noise from the fMRI timeseries, fMRI confounds generated with fMRIPrep were loaded using the `load_confound` (v. 0.6.4.) Python package. Six motion parameters, signals estimated from cerebrospinal fluid (CSF) and white matter (WM), their derivatives, quadratic terms, and squares of derivatives were regressed out from functional data separately for each run. The rs-fMRI data from each subject was smoothed with a full width at half maximum 6 mm Gaussian kernel, temporally bandpass filtered in the 0.01–0.1 Hz frequency range and spatially parcellated (400 parcels) according to the Schaefer atlas [30]. The Schaefer atlas was chosen for its basis in resting-state functional networks and its frequent use in previous functional connectome gradient studies.

Linear methods have been shown to offer better gradient reliability than non-linear alternatives [17]. For this reason, to estimate connectivity gradients, we applied generalised Canonical Correlation Analysis (gCCA) to all our subjects' timeseries using a Python implemented package `mvlearn` (<https://mvlearn.github.io/references/embed.html#generalized-canonical-correlation-analysis-gcca>). This decomposes the functional connectome into primary components, referred to as gradients, with each gradient explaining varying levels of variance in connectivity. These gradients discriminate across levels of the cortical hierarchy (i.e., sensory processing vs. higher-order cognition), whereas region specific values along the gradient, referred to as embedding values, reflect the similarity in connectivity along the sensory-transmodal axis. Further details on the connectome gradient mapping specific pipeline can be found in Supplementary Methods.

### Gradient mapping

We investigated principal and secondary gradient differences between FTD groups and controls. Each of the 400 brain parcels for which we extracted embedding values along the gradients belongs to a canonical functional network within the partition scheme described by Yeo and colleagues (Fig. 1) [31]. The present work focused on these two first functional gradients which each explaining a substantial portion of the data variance.

We performed a mixed effects model to compare principal and secondary gradient values for each parcel allocated to a given functional

network between controls and each FTD group. Thus, gradient scores for each parcel were included in the model as the dependent variable, while network label as well as group were entered as fixed effects. Subject, parcel label and acquisition protocol (accounting for site but also protocol differences) were entered as random effects. Finally, age and sex were also included in the model as fixed effects. We then investigated the Group  $\times$  Network interaction and performed post-hoc pairwise tests, comparing each network between controls and each FTD group. Resulting  $p$ -values were corrected for multiple comparisons including the three group comparisons and the 400 parcels using the Benjamini–Hochberg FDR correction.

### Assessing relationships between gradients, atrophy and disease severity

For each patient group, we also computed linear mixed effects models to assess the effect of atrophy on gradient values for each parcel, including age, sex and protocol as covariates into the model. We then investigated if the effect was significant for each network.

For each subject, networks' parcels' thickness and gradient values were averaged. To assess whether functional gradients or cortical atrophy was more correlated with disease severity (assessed by the MMSE), these average network gradient and atrophy scores were then correlated with MMSE scores using Spearman's correlations.

### Correlation of gradient changes with cognitive measures

To investigate the clinical relevance of altered connectome gradients in patients with bvFTD, we computed a summary metric of each gradient corresponding to the range between both extremes of the spectrum. The distance between the DMN and sensorimotor network along the principal gradient and the distance between the SN and visual network along the secondary gradient are a measure of differentiation/dedifferentiation of networks, whereby the shorter the distance (constriction of connectivity space) the less differentiated the networks.

We computed partial correlations between the miniSEA with these summary metrics in patients with bvFTD, accounting for disease duration (number of years since first symptoms) and severity (MMSE). As the direction of change of the secondary gradient extremes were different, with SN constricting and visual network expanding the axis in all patient groups, we also specifically correlated the SN and visual network embedding values with miniSEA scores in patients with bvFTD, also accounting for disease duration and severity. Due to the cognitive protocols across the sites not being harmonised and as the miniSEA task can be lengthy to administer, only a subset of patients were included in these analyses (Table 1).

All statistical tests were conducted in RStudio (v 4.2.0). Results on the cortical surface are presented using the opensource python package 'visbrain'.

## RESULTS

### Demographics and cognition

As demographic details did not significantly differ between the two sites for each participant group ( $p > 0.05$ ), these independently acquired datasets were merged for subsequent analyses. There were no significant demographic differences between patient groups and controls ( $p > 0.05$ ), except for patients with nfvPPA being older than the other patient groups ( $p < 0.02$ ) (Table 1). As expected, patient groups all had a significantly lower MMSE score than controls ( $p < 0.001$ ) (Table 1). Moreover, compared to controls, patients with bvFTD showed significantly reduced scores on the miniSEA ( $p < 0.0001$ ) (Table 1). Violin plots of patients with bvFTD and controls performance on the miniSEA are reported in Supplementary Fig. 2.

### Cortical thickness

Each clinical FTD group showed reduced cortical thickness compared to controls in expected regions. Thus, patients with bvFTD showed an average of around 10% reduction of cortical thickness compared to controls in bilateral medial prefrontal cortex, anterior cingulate cortex and middle temporal gyrus as well as around a 20% reduction in the bilateral anterior temporal

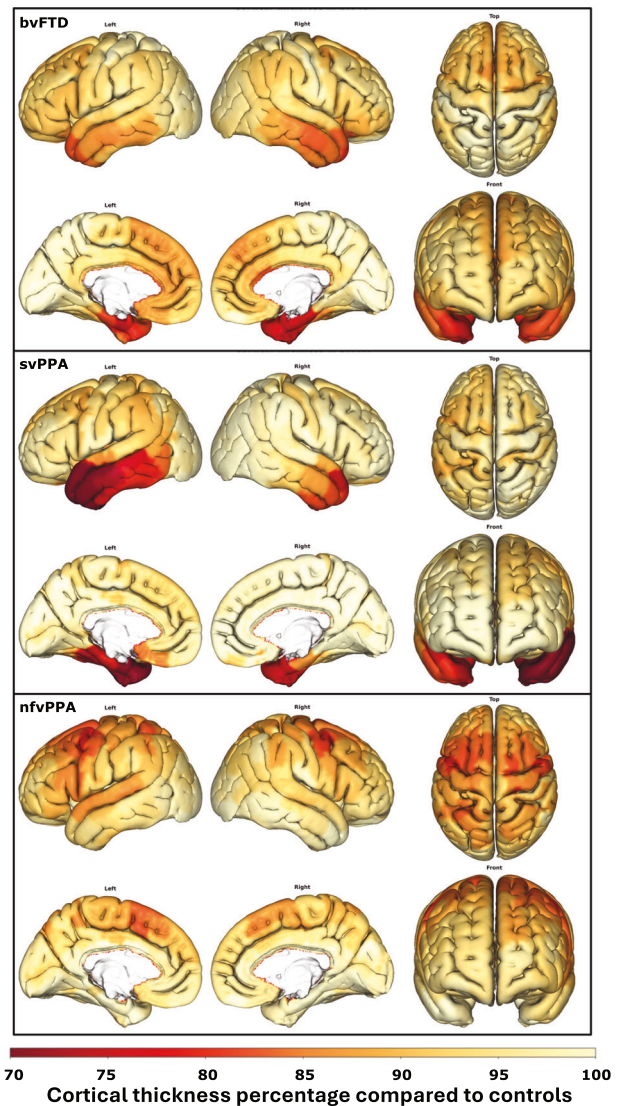


**Fig. 2 Grey matter atrophy.** Cortical thickness for each FTD group expressed as percentages of control means for each parcel. bvFTD behavioural variant FTD, svPPA semantic variant of Primary Progressive Aphasia, nfvPPA non-fluent variant of Primary Progressive Aphasia.

lobes and the frontoinsula region. Patients with svPPA showed reduced cortical thickness by up to 30% in left anterior temporal lobe, particularly the temporal pole, as well as up to around 25% in right temporal pole compared to controls. In nfvPPA, the pattern of reduced cortical thickness compared to controls was more widespread within the frontal and parietal lobes, involving up to 20% reductions within the supplementary motor area, particularly on the left, as well as up to 15% reduction in medial and inferior frontal cortex and left superior temporal gyrus (Fig. 2).

### Cortical gradients

In controls, the first two gradients explained a total of 48% of the variance; 29% and 19% respectively (Supplementary Fig. 3). There was no significant difference in the variance explained by each gradient between controls and the patient groups (Mann–Whitney-U,  $p < 0.05$ ). The principal gradient anchored sensorimotor areas at its positive extreme and DMN at its negative extreme (Fig. 3a), with a gradual transition from sensory to transmodal association networks similar to what has been reported in previous work [9]. Along our secondary gradient, the

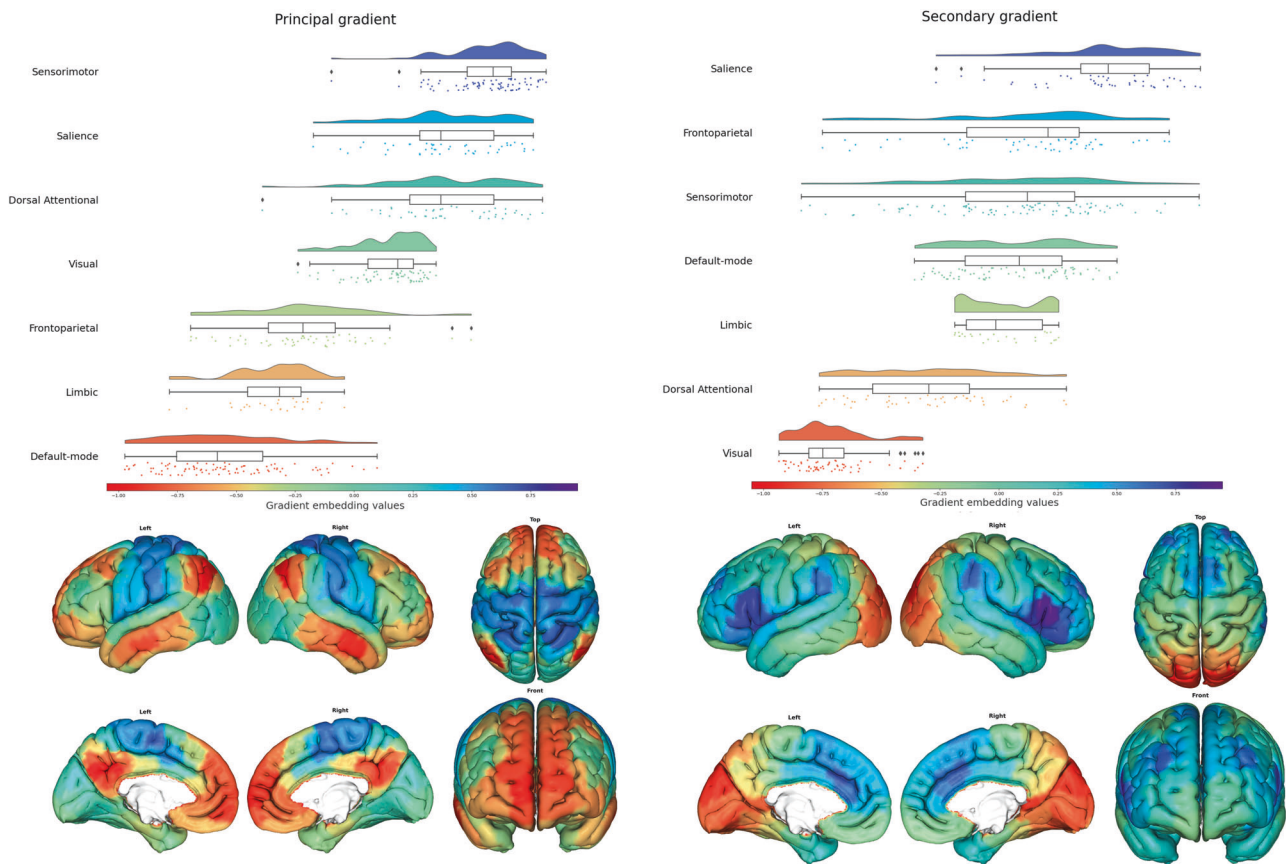


**Fig. 3 Principal and secondary gradients in controls.** Distribution of embedding values along the principal and secondary gradients for each canonical resting-state network in healthy controls, colour-coded according to Yeo et al., 2018 partition scheme. Below, the cortical surface is presented according to each parcel's average embedding value along the gradients. Along the principal gradient, the sensorimotor network is anchored on one end of the spectrum in dark blue/purple (precentral and postcentral gyri) and on the opposite end lies the default-mode network in bright red (posterior cingulate cortex/precuneus, medial prefrontal cortex, inferior parietal lobule). Along the secondary gradient, the saliency network is anchored on one end of the spectrum in dark blue/purple (anterior insula, anterior cingulate cortex) and on the opposite end lies the visual network in bright red (occipital lobe).

visual network occupied the negative extreme, while areas from the SN populated the positive end of this gradient (Fig. 3b). Brain regions with the highest or lowest embedding values are at the extremes of the axis, contributing most to the latent component and having the most differentiated functional connectivity. Regions with similar embedding values have similar connectivity patterns, and those near the centre (embedding value around 0) contribute less to the latent component.

Local alterations were notable, particularly widespread in patients with bvFTD and more focal in the language variants. Figure 4 reports results in patient populations. The distribution of patients for each network and along each gradient is presented in Supplementary Fig. 1.

#### Principal and secondary gradients group comparisons

The mixed models comparing groups on the principal and secondary gradient embedding values for each of the 400 parcels identified main effects of Network ( $p < 0.0001$ ) as well as significant Group  $\times$  Network interactions ( $p < 0.0001$ ). All  $p$ -values reported are corrected for multiple comparisons.

Pairwise comparisons at each network level found that patients with bvFTD showed significantly different principal gradient values within the DMN, the SN and visual network compared to controls ( $p < 0.0001$ ), their embedding values shifting towards the centre of the spectrum. Similarly, patients with nfvPPA showed significantly different principal gradient values within the DMN and sensorimotor network compared with controls ( $p < 0.0001$ ),

with both extreme-end networks' embedding values shifting towards the centre of the spectrum. Finally, patients with svPPA also showed significantly different principal gradient values within the limbic network ( $p < 0.0001$ ) and the sensorimotor compared to controls ( $p = 0.04$ ), again these networks' embedding values shifted towards the centre of the spectrum. Figure 5 (left) shows the adjusted embedding value means along the principal gradient for each functional network, grouped for each FTD variant. Controls' means are presented on the left for comparison. Details from the statistical model are presented in Supplementary Table 1.

All networks along the secondary gradient in patients with bvFTD showed significant differences compared to controls ( $p < 0.01$ ), with the largest changes occurring within the networks on either end of the spectrum, the SN and visual network ( $p < 0.0001$ ). Though the SN showed convergence towards the centre of the spectrum, the visual network expanded the axis by shifting away from the SN. Moreover, the middle networks' embedding values mostly shifted towards the SN end of the spectrum, apart from the DMN which shifted towards the visual end. Similarly, patients with nfvPPA showed significant changes along the secondary gradient with the same direction of changes of the SN and visual network as in patients with bvFTD compared to controls ( $p < 0.0001$ ). Moreover, patients with nfvPPA also showed a significant shift of the limbic ( $p = 0.03$ ) and sensorimotor network ( $p < 0.0001$ ) towards the SN and thus away from the visual network. Finally, patients with svPPA showed an expansion of the spectrum with visual network shifting away

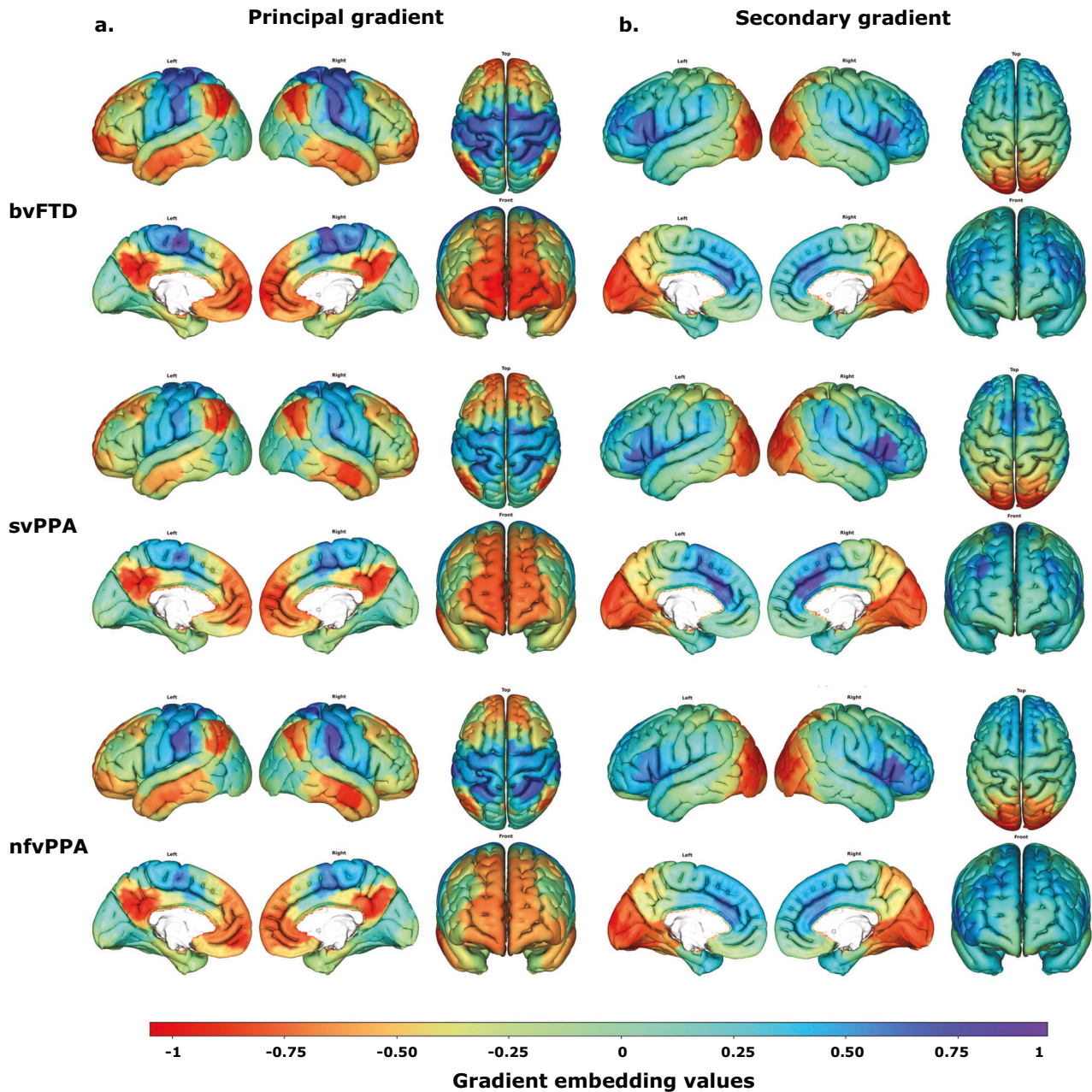


**Fig. 4 Gradients in the different FTD variants.** The cortical surface is presented according to each parcel's average embedding value along the principal (panel a) and secondary (panel b) gradient in each FTD variant group. bvFTD behavioural variant FTD, svPPA semantic variant of Primary Progressive Aphasia, nfvPPA non-fluent variant of Primary Progressive Aphasia.

from the SN ( $p < 0.0001$ ) whilst the limbic ( $p = 0.010$ ) and sensorimotor ( $p < 0.0001$ ) networks' embedding values significantly shifted along the secondary gradient, towards the SN. Figure 5 (right) shows the adjusted embedding value means along the principal gradient for each functional network, grouped for each FTD variant. Controls' means are presented on the left for comparison.

Figure 6 presents an overview of the distribution of the embedding values along the principal (left) and secondary (right) gradient, grouped according to functional network with a distribution plot for each FTD variant and controls. More detailed results from the statistical comparisons are presented in Supplementary Table 1.

To ensure that within-group heterogeneity did not impact the results, we performed the same mixed model analyses a)

excluding the genetic cases from the bvFTD and nfvPPA groups and b) comparing the PPA groups with only controls from site 2 as these patients were only from site 2. These control analyses did not show major differences (see Supplementary Tables 2 and 3).

#### Relationships between gradients, atrophy and disease severity

Supplementary Table 4 summarises the significant effects of cortical thickness on both the principal and secondary gradients for each network and within each patient group. In patients with bvFTD, there was a significant effect of atrophy within the limbic network and SN principal gradient ( $p = 0.001$ ;  $p < 0.001$ ) and within the DMN secondary gradient ( $p = 0.015$ ). In patients with svPPA, there was a significant effect of atrophy within the SN principal gradient ( $p < 0.001$ ) and marginally significant effects

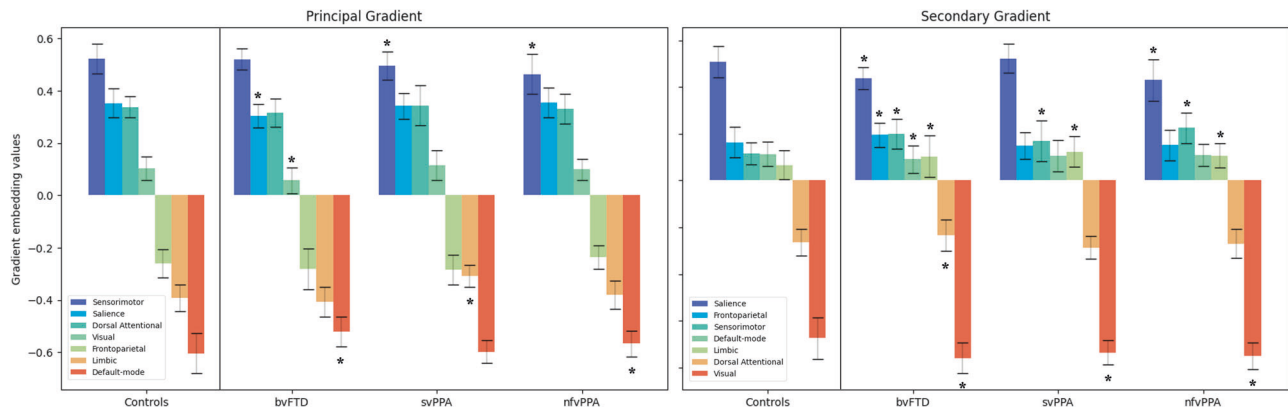


**Fig. 5 Network differences between groups along each gradient.** Bar plot with error bars of average principal (left) and secondary (right) gradients for each group and for each network, colour-coded according to their position along each gradient axis. \* indicate significant differences for each network, between the patient group and controls who are presented on the left in both graphs ( $p < 0.05$ , corrected for multiple comparisons). bvFTD behavioural variant FTD, svPPA semantic variant of Primary Progressive Aphasia, nfvPPA non-fluent variant of Primary Progressive Aphasia.

within the limbic and visual networks ( $p = 0.05$ ). In patients with nfvPPA, there was a significant effect of atrophy within the dorsal attentional network, frontoparietal network, SN and visual network principal gradient ( $p = 0.04$ ;  $p = 0.006$ ;  $p = 0.05$ ;  $p = 0.001$ ) and within the dorsal attentional network, DMN and limbic network secondary gradient ( $p = 0.002$ ;  $p < 0.001$ ;  $p < 0.001$ ).

In patients with bvFTD, only the DMN principal gradient was significantly negatively correlated with MMSE scores ( $\rho = -0.40$ ;  $p = 0.03$ ). In patients with svPPA, only frontoparietal network cortical thickness was significantly positively correlated with MMSE scores ( $\rho = 0.55$ ;  $p = 0.04$ ). Finally, in patients with nfvPPA, MMSE was significantly positively correlated with the cortical thickness within the DMN ( $\rho = 0.56$ ;  $p = 0.03$ ), limbic network ( $\rho = 0.65$ ;  $p = 0.009$ ) and frontoparietal network ( $\rho = 0.59$ ;  $p = 0.02$ ) as well as with secondary gradient embedding values of dorsal attentional network ( $\rho = 0.56$ ;  $p = 0.03$ ), DMN ( $\rho = -0.66$ ;  $p = 0.007$ ), and visual network ( $\rho = 0.59$ ;  $p = 0.03$ ). Supplementary Table 5 summarises these results.

#### Clinical relevance of principal and secondary gradients

We found a significant positive correlation ( $r = 0.40$ ,  $p = 0.05$ ) between the principal gradient range and social cognition performances (miniSEA) in patients with bvFTD. Similarly, the secondary gradient range showed a trend towards a positive correlation ( $r = 0.42$ ,  $p = 0.08$ ). In both cases, the more constricted the gradient, the worse the score on the miniSEA (Fig. 7a). Visual network was significantly negatively correlated with social cognition scores ( $r = -0.58$ ,  $p = 0.011$ ). In this case, the more the visual network embedding values were expanding the axis (smaller values), the better the score on the miniSEA (Fig. 7b). Figure 7 presents the simple correlation plots for interpretability. The partial correlation plots are reported in Supplementary Fig. 4.

#### DISCUSSION

In the present study, we used connectome gradient mapping to investigate macroscale functional network organisation in low dimensional space in patients affected by FTD. Healthy control subjects exhibited a typical hierarchy and differentiation of functional network connectivity patterns. The principal gradient captured a progressive hierarchy between sensorimotor regions (processing external stimuli) on one side and transmodal association regions (internal processes, like mind-wandering) on the other, consistent with previous findings [9]. This differentiation supports efficient external vs. internal processing. The secondary gradient sharply distinguished the SN and visual network,

reflecting a separation between regions attending to external visual cues and those interpreting their social relevance, thus dissociating observed vs. predicted states. This aligns with recent studies showing a SN-visual axis in healthy controls [32] and a transmodal network, like the DMN, opposite the visual network along the secondary gradient [14]. These principal and secondary gradients explained 48% of the variance within the data, capturing a healthy hierarchy that enables the transition from concrete perception to abstract cognition, the basis of the evolutionary transition from apes to humans and of higher-order cognitive and behavioural functions [33].

In all patients with FTD, although broad gradients were maintained, network organisation was perturbed. Along the principal gradient, extreme-end networks shifted towards the centre, causing a constriction of FC space across the FTD spectrum, with focal changes in sensorimotor and limbic networks in patients with PPA. While the secondary gradient also showed these specific alterations in patients with PPA, it presented notable widespread changes in patients with bvFTD. Interestingly, the secondary gradient also revealed a common pattern in all FTD patient groups with the visual network expanding the axis.

#### Principal gradient – marker of neurodegeneration

Across all patient groups, the principal gradient was significantly constricted, whereby networks positioned at the extreme-ends of the spectrum (DMN and sensorimotor) shifted towards the centre compared to controls. This suggests that these networks' FC patterns become more similar to other networks', losing their specificity, a process known as *dedifferentiation*. Consequently, these networks may activate in situations where they normally would not or fail to activate where they should. Previous work in psychiatric or non-neurodegenerative neurological patients have shown such principal gradient constrictions [12, 15]. We are the first to demonstrate this *dedifferentiation* in neurodegenerative diseases. *Dedifferentiation* is most likely a mechanism common to many brain dysfunctions related to neurological conditions.

In this paper, we measured network *dedifferentiation* as the distance between the extreme-ends of the gradient representing overall constriction of FC space. In our patients with bvFTD, principal gradient constriction mainly depended on the shift of the DMN towards the centre and correlated with poorer social cognition scores (miniSEA). Social cognition dysfunction, one of the hallmark clinical disturbances in bvFTD, relies on maintaining a clear dissociation between external (sensorimotor) and internal (DMN) processing. As with the miniSEA, DMN FC changes in bvFTD significantly correlated also with a lower MMSE. Surprisingly,

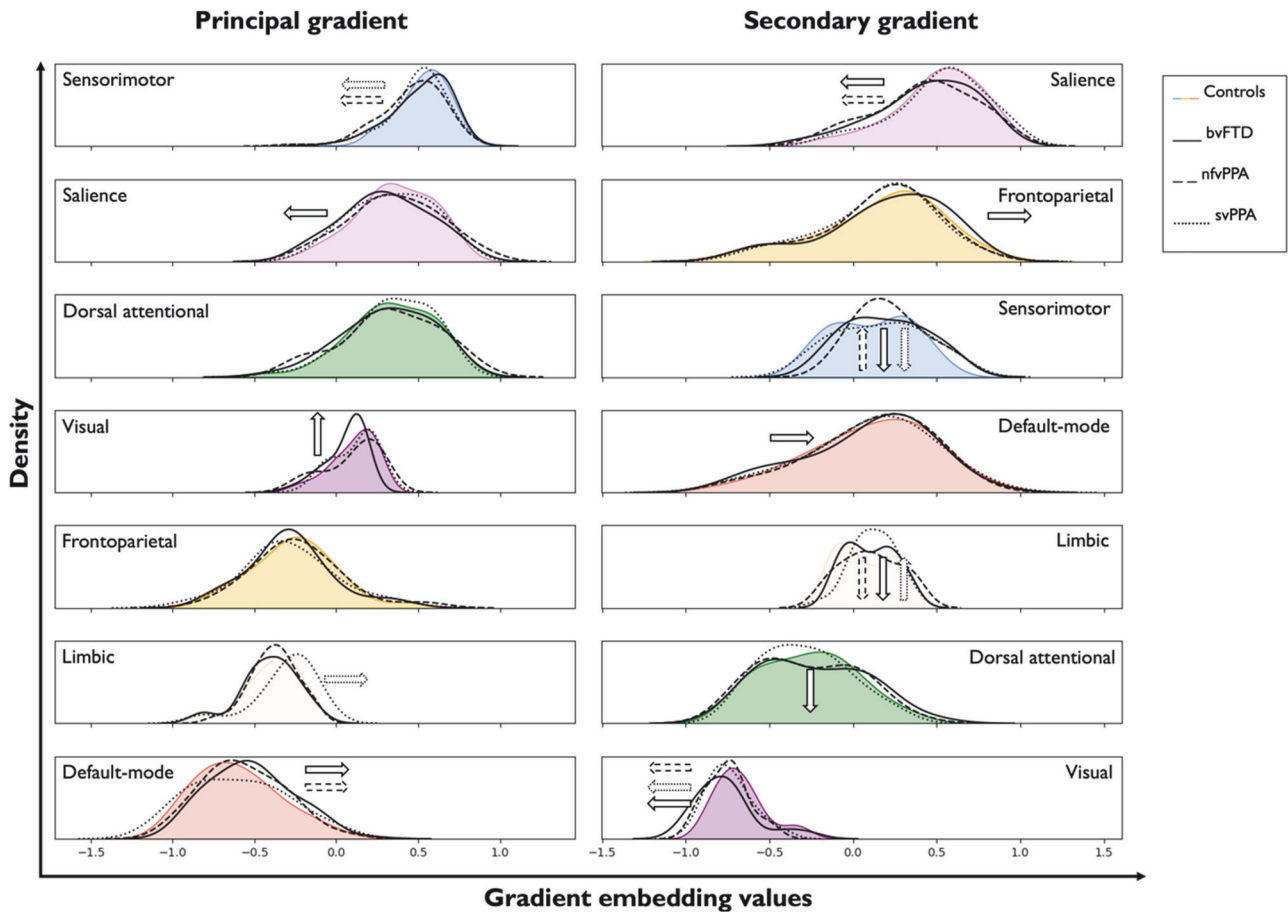


**Fig. 6 Distribution of gradient embedding values for each network and for each group.** Controls' density plot colour-coded according to Yeo et al., 2018 partition scheme. Arrows indicate significant shift along the gradient for each group. bvFTD patients' density plot/arrow in solid black line, nfvPPA patients' density plot/arrow in dashed black line and svPPA patients' density plot/arrow in dotted black line. bvFTD behavioural variant FTD, svPPA semantic variant of Primary Progressive Aphasia, nfvPPA non-fluent variant of Primary Progressive Aphasia.

atrophy was not correlated with MMSE, highlighting the particular contribution of altered FC to bvFTD clinical picture.

#### Widespread alterations in bvFTD

In patients with bvFTD, along both gradients, we observed the SN shifting towards the DMN, thus reducing the differentiation between these networks' respective activity. A decrease of SN FC in bvFTD is one of the most replicated findings in the field [7, 34–44]. It is believed the frontoinsula and anterior cingulate cortex, SN hubs, are rich of von Economo neurons and fork cells and, for this reason, particularly vulnerable to FTD pathology [45, 46]. Anatomically, these regions are the most vulnerable to grey matter degeneration. This explains why SN atrophy also contributed significantly to gradient values. Looking beyond regions of atrophy, changes in the interplay between the DMN and SN have been linked to symptoms in patients with bvFTD [34, 37, 47, 48]. Our findings of reduced differentiation between these networks support a model where the SN and DMN are anticorrelated, exerting inhibitory influence on each other, crucial for responding to prevailing goals and conditions [34, 49].

Some previous work has pointed towards FC changes extending beyond DMN/SN showing the interplay between many other networks is affected in bvFTD [7]. In line with this, along the secondary gradient, we observe that all seven functional networks showed significant shifts in bvFTD, even at relatively early stages of the disease (average disease duration of 3–6 years). Conversely, PPA patient groups did not show such striking widespread changes. It is likely that for patients with PPA, the interplay

between networks plays a less important role, related to the more focal nature of brain damage, and associated proteinopathies.

#### Focal alterations in PPA

FC studies in patients with PPA are sparse, mostly reporting specific local frontotemporal or subcortical structure disconnections [50–53] with few investigating macroscale functional network changes. Along both gradients, PPA variants exhibited specific alterations within sensorimotor and limbic networks, with larger changes of the former in patients with nfvPPA and of the latter in svPPA. These functional changes are likely to be related to key areas of structural changes, such as motor language related cortices in nfvPPA [54–57] and limbic structures in svPPA [39]. Importantly, however, we highlight that atrophy within sensorimotor and limbic networks did not contribute significantly to these networks' gradient values, supporting a specific role for functional changes in these patient groups. The specific contribution of FC to svPPA clinical picture has already been reported for the limbic network [58, 59].

When investigating the changes more thoroughly, we noticed that in our controls both sensorimotor and limbic networks were bimodally distributed along the secondary gradient, thus dissociating regions with differing patterns of FC. This bimodal distribution is lost in patients with PPA, in sensorimotor network for nfvPPA and in limbic network for svPPA. The 17-network parcellation described by Yeo and colleagues divides the sensorimotor strip into dorsal and ventral subnetworks, with the boundary between these roughly positioned between the hand



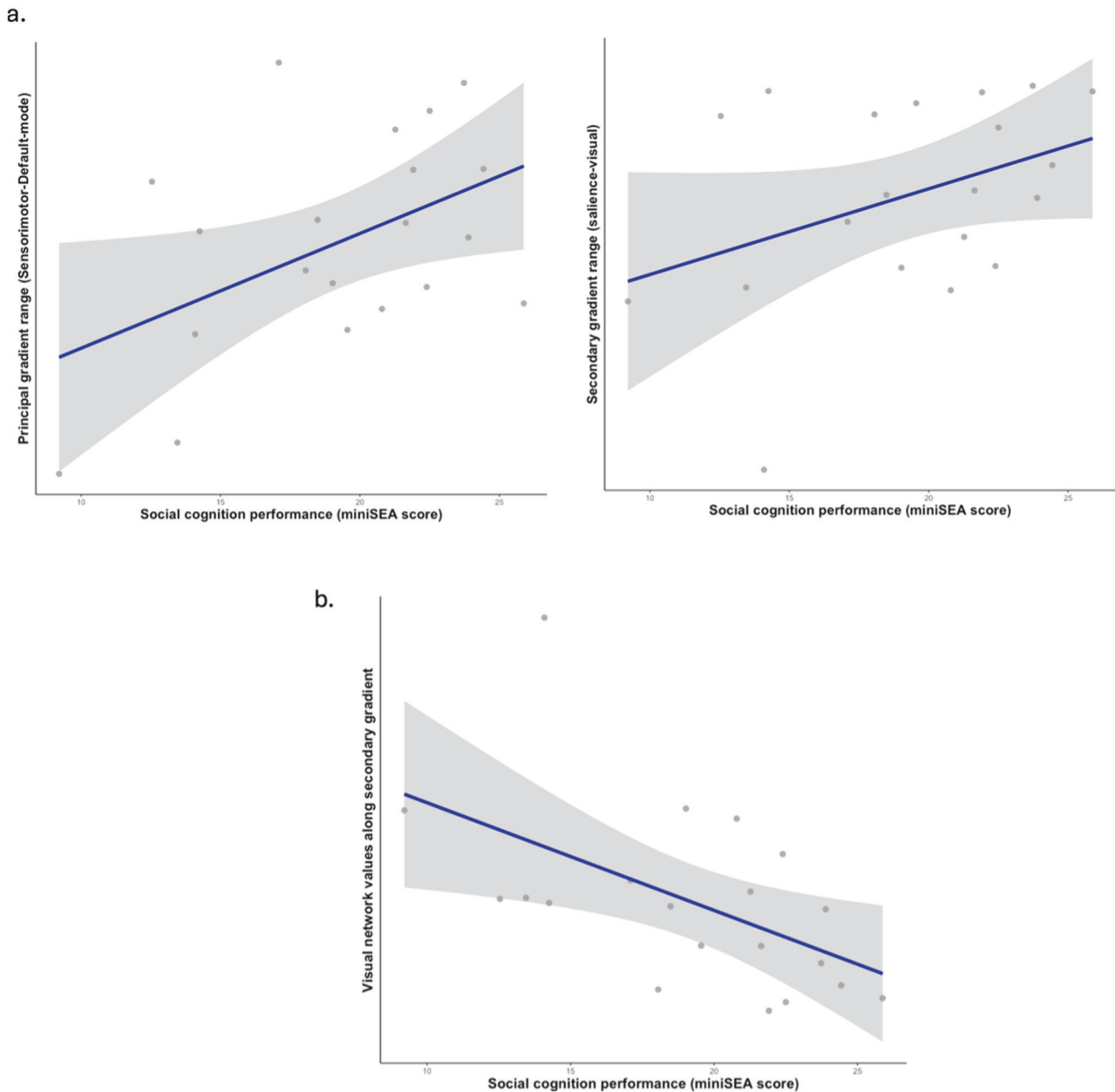


**Fig. 7 Correlations between social cognition and gradients.** **a** Partial correlations between mini-Social cognition & Emotional Assessment battery (miniSEA) scores with the principal gradient (left;  $r = 0.40$ ,  $p = 0.05$ , uncorrected) and secondary gradient (right;  $r = 0.42$ ,  $p = 0.080$ , uncorrected) range, accounting for disease severity (MMSE) and duration (number of years since first symptoms) in patients with bvFTD. The smaller the gradients' range (constriction), the worse the miniSEA scores. **b** Partial correlation between miniSEA scores and the secondary gradient visual network ( $r = -0.42$ ;  $p = 0.011$ , uncorrected). The smaller the visual network embedding values, expanding the axis, the better the score on the miniSEA. DMN default-mode network, miniSEA mini-Social cognition & Emotional Assessment.

and tongue representations [31]. The bimodal distribution of sensorimotor network may dissociate sets of body part representations, and the high kurtosis found in patients with nvPPA could represent a blurring of this boundary. The loss of this bimodal representation might in our case correspond to an example of *dedifferentiation* at a more local level, within sensorimotor network, and potentially relating to the specific oro-facial symptoms characteristic of this patient group [19]. Similarly, Yeo's 17-network parcellation dissociates the limbic network into two subnetworks, orbitofrontal cortex and temporal pole, which may underlie the bimodal distribution observed in controls. As atrophy in svPPA is particularly pronounced in temporal pole and less so in orbitofrontal cortex, the smoothing of the bimodal distribution

may also be a result of this pattern of atrophy. Thus, our findings of specific FC alterations in sensorimotor and limbic network in patients with nvPPA and svPPA are novel and warrant further investigation. Understanding the specific patterns of these networks, their relationship to function and their potential use as a functional signature in these patients is crucial.

#### Visual network functional compensation?

In all three patient groups, the visual network shifted outwards along the secondary gradient, expanding the axis. As functional networks' activities are correlated and anticorrelated with one another, this change in visual network FC could reflect over-excitation caused by reduced inhibitory control from other

networks as they accrue pathology and undergo atrophy, such as SN [36, 37]. In line with this, the SN's FC pattern was significantly altered in both patients with bvFTD and nvPPA and previous work has alluded to the SN's reduced inhibitory control contributing to aberrant judgment and behaviour in bvFTD patients [60]. Another hypothesis is that visual network FC changes are a compensatory mechanism to maintain neural differentiation between predicted vs. observed processes. This is supported by visual network secondary gradient values significantly correlating with miniSEA scores in patients with bvFTD. A previous study demonstrated that patients with bvFTD increased fixations towards emotional faces to facilitate the contextualisation of emotional information [61]. This behavioural compensatory mechanism would presumably lead to visual network FC changes, such as those reported in our work.

### Atrophy and functional connectivity

Atrophy and FC are undeniably closely related [45]. Our findings of DMN and SN changes are consistent with grey matter hubs of atrophy in bvFTD [62] with up to 20–30% grey matter volume reductions in regions within these networks in patients with bvFTD compared to controls. Similarly, our observed changes within sensorimotor and limbic network in nvPPA and svPPA align with their respective atrophy patterns within sensorimotor cortices and orbitofrontal cortex/temporal poles [19]. However, our study highlights that atrophy patterns do not perfectly overlap with functional network changes [63]. This is further emphasised by finding that atrophy did not contribute specifically to the networks which showed gradient differences compared to controls. For example, in patients with bvFTD, along the secondary gradient, all seven networks were impacted but atrophy only within the DMN contributed. Thus, functional network changes do not seem to be fully explained by atrophy alone in any FTD subtype [64]. The finding that functional changes are more extensive than structural suggests that functional alterations may possibly be at the origin of symptoms, only later followed by structural changes.

We conducted additional analyses to evaluate the correlation of gradient and cortical thickness to disease severity, as measured by MMSE. In patients with bvFTD, FC measured within the DMN correlated inversely with MMSE. In nvPPA both cortical thickness and FC correlated with MMSE. Finally, in svPPA only cortical thickness correlated with MMSE. These results suggest that within the spectrum of FTD, underlying proteinopathy, which differs among clinical phenotypes, seems to preferentially affect different brain features (grey matter and/or FC).

Interestingly, recent work has suggested that the longitudinal spread of atrophy can be predicted using an individual's functional connectome [65]. Brown et al. found that the shortest path length in FC space to the epicenter, combined with quantifying atrophy within a region's network neighbours, accurately estimated the spatial pattern of subsequent atrophy in patients with bvFTD and svPPA. This highlights the utility of FC profiles in predicting atrophy progression. However, the onset, evolution and relationship of pathological structural and functional changes in FTD are not fully understood, even at the group level, as studies have lacked multimodal longitudinal data [66].

### Limitations

The present work has some limitations. Firstly, the associations of our functional gradient results with clinical and cognitive measures warrant further validation. Due to our limited sample size, particularly in the PPA variants, we were not able to extensively investigate the relationships between cognition/behaviour and functional gradients. Moreover, the miniSEA was unfortunately only available for half our bvFTD patients, limiting our interpretations. Finally, due to combining data from two sites, we were limited to cognitive and clinical tests which were in

common across both cohorts. Thus, we chose the MMSE for assessing disease severity, however, we acknowledge that is not the ideal test for patients with FTD.

A second limitation is that the secondary gradient we present did not follow the "prototypical" secondary gradient first described by Margulies et al. [9]. Moreover, healthy controls showed large variability of embedding values within one same network. Others have reported similar gradients to ours [14, 32] and there are several factors which may explain these differences. Firstly, our sample's average age is older than in most studies (controls were 67 years old on average), and gradients have been shown to change across the lifespan [15, 67]. Additionally, our method of extracting gradients using a linear approach is not the same as in previous work [9]. Linear methods have the advantage of producing better gradient reliability and by applying the dimension reduction directly to the timeseries, we directly address group-level consistency and do not require thresholding of functional connectivity matrices [17]. As this is the first study to explore functional gradients in patients with FTD (and one of the first in neurodegenerative diseases), and in view of our interesting secondary gradient findings, it will be important for these to be replicated in other samples.

A final limitation of the study is that the subcortical structures or the basal ganglia are not included in resting-state functional networks described in this work, making our results limited to cortical networks.

### Concluding remarks and perspectives

In conclusion, gradient mapping offers a lens through which to characterise macroscale functional network organisation and relationships, essential for brain function. While specific network changes occur, this whole-brain, low-dimensional approach revealed widespread disruptions of the evolutionarily derived global network hierarchy in each FTD variant. Dissociations between internal/external processes, as well as between predicted/observed processes were significantly altered in these patients. Our secondary gradient may be a specific marker for bvFTD because it was so majorly impacted. As molecular nexopathies, correlating such FC profiles with underlying molecular pathologies is crucial to understanding the clinico-anatomical heterogeneity found amongst patients with FTD [68]. Refining these findings could help identify the specific role FC can play in disease detection, differential diagnosis and measuring disease progression in FTD.

Future research should focus on developing reliable FC profiles using connectome gradient mapping, particularly through longitudinal studies. Although methodological parameters require further optimisation, existing research indicates that low-dimensional connectivity gradients may outperform other approaches in predicting clinical scores and could serve as reproducible biomarkers. This potential, however, needs further investigation in the context of FTD.

Finally, if FC changes indeed precede brain atrophy, as some studies suggest, FC measures could serve as effective tools for patient stratification and for assessing the efficacy of disease-modifying therapies within a dynamic biomarker framework. Given that up to 30% of FTD cases are attributed to autosomal dominant genetic mutations [69], assessing FC gradients in presymptomatic individuals with these mutations would provide a valuable opportunity for early intervention and monitoring.

### DATA AVAILABILITY

Data from participants who agreed to the public distribution of data are available from the corresponding author upon reasonable request, while maintaining the anonymity of the participants.

## REFERENCES

- Felleman DJ, Van Essen DC. Distributed hierarchical processing in the primate cerebral cortex. *Cereb Cortex* N Y N. 1991;1:1–47.
- Mesulam MM. Large-scale neurocognitive networks and distributed processing for attention, language, and memory. *Ann Neurol*. 1990;28:597–613.
- Biswal B, Zerrin Yetkin F, Haughton VM, Hyde JS. Functional connectivity in the motor cortex of resting human brain using echo-planar mri. *Magn Reson Med*. 1995;34:537–41.
- Friston KJ. Functional and effective connectivity in neuroimaging: A synthesis. *Hum Brain Mapp*. 1994;2:56–78.
- Fox MD, Snyder AZ, Vincent JL, Corbetta M, Van Essen DC, Raichle ME. The human brain is intrinsically organized into dynamic, anticorrelated functional networks. *Proc Natl Acad Sci*. 2005;102:9673–8.
- DeSerisy M, Ramphal B, Pagliaccio D, Raffanella E, Tau G, Marsh R, et al. Frontoparietal and default mode network connectivity varies with age and intelligence. *Dev Cogn Neurosci*. 2021;48:100928.
- Ferreira LK, Lindberg O, Santillo AF, Wahlund LO. Functional connectivity in behavioral variant frontotemporal dementia. *Brain Behav*. 2022;12:e2790.
- Ng ASL, Wang J, Ng KK, Chong JSX, Qian X, Lim JKW, et al. Distinct network topology in Alzheimer's disease and behavioral variant frontotemporal dementia. *Alzheimers Res Ther*. 2021;13:13.
- Margulies DS, Ghosh SS, Goulas A, Falkiewicz M, Huntenburg JM, Langs G, et al. Situating the default-mode network along a principal gradient of macroscale cortical organization. *Proc Natl Acad Sci*. 2016;113:12574–9.
- Bayrak, Khalil AA, Villringer K, Fiebach JB, Villringer A, Margulies DS, et al. The impact of ischemic stroke on connectivity gradients. *NeuroImage Clin*. 2019;24:101947.
- Hong SJ, Vos de Wael R, Bethlehem RAI, Lariviere S, Paquola C, Valk SL, et al. Atypical functional connectome hierarchy in autism. *Nat Commun*. 2019;10:1022.
- Meng Y, Yang S, Chen H, Li J, Xu Q, Zhang Q, et al. Systematically disrupted functional gradient of the cortical connectome in generalized epilepsy: Initial discovery and independent sample replication. *NeuroImage*. 2021;230:117831.
- Wang J, Zhou Y, Ding J, Xiao J. Functional gradient alteration in individuals with cognitive vulnerability to depression. *J Psychiatr Res*. 2021;144:338–44.
- Pasquini L, Fryer SL, Eisendrath SJ, Segal ZV, Lee AJ, Brown JA, et al. Dysfunctional Cortical Gradient Topography in Treatment-Resistant Major Depressive Disorder. *Biol Psychiatry Cogn Neurosci Neuroimaging*. 2023;8:928–39.
- Dong D, Luo C, Guell X, Wang Y, He H, Duan M, et al. Compression of Cerebellar Functional Gradients in Schizophrenia. *Schizophr Bull*. 2020;46:1282–95.
- Koen JD, Rugg MD. Neural Dedifferentiation in the Aging Brain. *Trends Cogn Sci*. 2019;23:547–59.
- Hong SJ, Xu T, Nikolaidis A, Smallwood J, Margulies DS, Bernhardt B, et al. Toward a connectivity gradient-based framework for reproducible biomarker discovery. *NeuroImage*. 2020;223:117322.
- Rascovsky K, Hodges JR, Knopman D, Mendez MF, Kramer JH, Neuhaus J, et al. Sensitivity of revised diagnostic criteria for the behavioural variant of frontotemporal dementia. *Brain*. 2011;134:2456–77.
- Gorno-Tempini ML, Hillis AE, Weintraub S, Kertesz A, Mendez M, Cappa SF, et al. Classification of primary progressive aphasia and its variants. *Neurology*. 2011;76:1006–14.
- Warren JD, Rohrer JD, Hardy J. Disintegrating brain networks: from syndromes to molecular nexopathies. *Neuron*. 2012;73:1060–2.
- Zhou J, Liu S, Ng KK, Wang J. Applications of Resting-State Functional Connectivity to Neurodegenerative Disease. *Neuroimaging Clin*. 2017;27:663–83.
- Filippi M, Basaia S, Canu E, Imperiale F, Meani A, Caso F, et al. Brain network connectivity differs in early-onset neurodegenerative dementia. *Neurology*. 2017;89:1764–72.
- Agosta F, Canu E, Sarro L, Comi G, Filippi M. Neuroimaging findings in frontotemporal lobar degeneration spectrum of disorders. *Cortex*. 2012;48:389–413.
- Batrancourt B, Lecouturier K, Ferrand-Verdejo J, Guillemot V, Azuar C, Bendetowicz D, et al. Exploration Deficits Under Ecological Conditions as a Marker of Apathy in Frontotemporal Dementia. *Front Neurol*. 2019;10. Available from: <https://www.frontiersin.org/articles/10.3389/fneur.2019.00941/full>.
- Russell LL, Greaves CV, Convery RS, Nicholas J, Warren JD, Kaski D, et al. Novel instructionless eye tracking tasks identify emotion recognition deficits in frontotemporal dementia. *Alzheimers Res Ther*. 2021;13:39.
- Bertoux M, Volle E, Funkiewiez A, Souza LC, de Leclercq D, et al. Social Cognition and Emotional Assessment (SEA) is a Marker of Medial and Orbital Frontal Functions: A Voxel-Based Morphometry Study in Behavioral Variant of Frontotemporal Degeneration. *J Int Neuropsychol Soc*. 2012;18:972–85.
- Esteban O, Markiewicz CJ, Blair RW, Moodie CA, Isik AI, Erramuzpe A, et al. fMRIPrep: a robust preprocessing pipeline for functional MRI. *Nat Methods*. 2019;16:111–6.
- Faskowitz J. faskowitz/multiAtlasTT v0.1 (v0.0.1). Zenodo; 2021. Available from: <https://doi.org/10.5281/zenodo.4459737>.
- Power JD, Barnes KA, Snyder AZ, Schlaggar BL, Petersen SE. Spurious but systematic correlations in functional connectivity MRI networks arise from subject motion. *NeuroImage*. 2012;59:2142–54.
- Schaefer A, Kong R, Gordon EM, Laumann TO, Zuo XN, Holmes AJ, et al. Local-Global Parcellation of the Human Cerebral Cortex from Intrinsic Functional Connectivity MRI. *Cereb Cortex*. 2018;28:3095–114.
- Yeo BTT, Krienen FM, Sepulcre J, Sabuncu MR, Lashkari D, Hollinshead M, et al. The organization of the human cerebral cortex estimated by intrinsic functional connectivity. *J Neurophysiol*. 2011;106:1125–65.
- Zheng C, Zhao W, Yang Z, Guo S. Initiative for the ADN. Functional connectome hierarchy dysfunction in Alzheimer's disease and its relationship with cognition and gene expression profiling. *J Neurosci Res*. 2024;102:e25280.
- Levy R. The prefrontal cortex: from monkey to man. *Brain*. 2024;147:794–815.
- Zhou J, Greicius MD, Gennatas ED, Growdon ME, Jang JY, Rabinovici GD, et al. Divergent network connectivity changes in behavioural variant frontotemporal dementia and Alzheimer's disease. *Brain*. 2010;133:1352–67.
- Filippi M, Agosta F, Scola E, Canu E, Magnani G, Marcone A, et al. Functional network connectivity in the behavioral variant of frontotemporal dementia. *Cortex*. 2013;49:2389–401.
- Agosta F, Sala S, Valsasina P, Meani A, Canu E, Magnani G, et al. Brain network connectivity assessed using graph theory in frontotemporal dementia. *Neurology*. 2013;81:134–43.
- Caminiti SP, Canessa N, Cerami C, Dodich A, Crespi C, Iannaccone S, et al. Affective mentalizing and brain activity at rest in the behavioral variant of frontotemporal dementia. *NeuroImage Clin*. 2015;9:484–97.
- Borroni B, Grassi M, Premi E, Gazzina S, Alberici A, Cosseddu M, et al. Neuroanatomical correlates of behavioural phenotypes in behavioural variant of frontotemporal dementia. *Behav Brain Res*. 2012;235:124–9.
- Farb NAS, Grady CL, Strother S, Tang-Wai DF, Masellis M, Black S, et al. Abnormal network connectivity in frontotemporal dementia: Evidence for prefrontal isolation. *Cortex*. 2013;49:1856–73.
- Lee SE, Khazenzon AM, Trujillo AJ, Guo CC, Yokoyama JS, Sha SJ, et al. Altered network connectivity in frontotemporal dementia with C9orf72 hexanucleotide repeat expansion. *Brain*. 2014;137:3047–60.
- Rytty R. Resting-state functional MRI in behavioral variant of frontotemporal dementia. 2016. <https://www.semanticscholar.org/paper/Resting-state-functional-MRI-in-behavioral-variant-Rytty/9a3e8e09cf91c9004284719ba131e80acad1ee5b>.
- Premi E, Cauda F, Gasparotti R, Diano M, Archetti S, Padovani A, et al. Multimodal fMRI Resting-State Functional Connectivity in Granulin Mutations: The Case of Fronto-Parietal Dementia. *PLOS ONE*. 2014;9:e106500.
- Hafkemeijer A, Möller C, Dopfer EGP, Jiskoot LC, Schouten TM, van Swieten JC, et al. Resting state functional connectivity differences between behavioral variant frontotemporal dementia and Alzheimer's disease. *Front Hum Neurosci*. 2015;9. Available from: <https://www.frontiersin.org/articles/10.3389/fnhum.2015.00474/full>.
- Moguilner S, García AM, Mikulan E, Hesse E, García-Cordero I, Melloni M, et al. Weighted Symbolic Dependence Metric (wSDM) for fMRI resting-state connectivity: A multicentric validation for frontotemporal dementia. *Sci Rep*. 2018;8:11181.
- Seeley WW, Crawford RK, Zhou J, Miller BL, Greicius MD. Neurodegenerative Diseases Target Large-Scale Human Brain Networks. *Neuron*. 2009;62:42–52.
- Seeley WW, Zhou J, Kim EJ. Frontotemporal Dementia: What Can the Behavioral Variant Teach Us about Human Brain Organization? *The Neuroscientist*. 2012;18:373–85.
- Rijpmma MG, Yang WFZ, Toller G, Battistella G, Sokolov AA, Sturm VE, et al. Influence of periaqueductal gray on other salience network nodes predicts social sensitivity. *Hum Brain Mapp*. 2022;43:1694–709.
- Sedeño L, Couto B, García-Cordero I, Melloni M, Baez S, Sepúlveda JPM, et al. Brain Network Organization and Social Executive Performance in Frontotemporal Dementia. *J Int Neuropsychol Soc*. 2016;22:250–62.
- Sturm VE, Brown JA, Hua AY, Lwi SJ, Zhou J, Kurth F, et al. Network Architecture Underlying Basal Arteriovenous Outflow: Evidence from Frontotemporal Dementia. *J Neurosci*. 2018;38:8943–55.
- Bonakdarpour B, Rogalski EJ, Wang A, Sridhar J, Mesulam MM, Hurley RS. Functional connectivity is reduced in early stage primary progressive aphasia when atrophy is not prominent. *Alzheimer Dis Assoc Disord*. 2017;31:101–6.
- Reyes P, Ortega-Merchan MP, Rueda A, Uriza F, Santamaria-García H, Rojas-Serrano N, et al. Functional Connectivity Changes in Behavioral, Semantic, and Nonfluent Variants of Frontotemporal Dementia. *Behav Neurol*. 2018;2018:e9684129.
- Botha H, Utianski RL, Whitwell JL, Duffy JR, Clark HM, Strand EA, et al. Disrupted functional connectivity in primary progressive apraxia of speech. *NeuroImage Clin*. 2018;18:617–29.
- Agosta F, Galantucci S, Valsasina P, Canu E, Meani A, Marcone A, et al. Disrupted brain connectome in semantic variant of primary progressive aphasia. *Neurobiol Aging*. 2014;35:2646–55.

54. Josephs KA, Duffy JR, Strand EA, Machulda MM, Senjem ML, Gunter JL, et al. The evolution of primary progressive apraxia of speech. *Brain*. 2014;137:2783–95.
55. Botha H, Duffy JR, Whitwell JL, Strand EA, Machulda MM, Schwarz CG, et al. Classification and clinicoradiologic features of primary progressive aphasia (PPA) and apraxia of speech. *Cortex*. 2015;69:220–36.
56. Mandelli ML, Caverzasi E, Binney RJ, Henry ML, Lobach I, Block N, et al. Frontal White Matter Tracts Sustaining Speech Production in Primary Progressive Aphasia. *J Neurosci*. 2014;34:9754–67.
57. Agosta F, Ferraro PM, Canu E, Copetti M, Galantucci S, Magnani G, et al. Differentiation between Subtypes of Primary Progressive Aphasia by Using Cortical Thickness and Diffusion-Tensor MR Imaging Measures. *Radiology*. 2015;276:219–27.
58. Yang WFZ, Toller G, Shdo S, Kotz SA, Brown J, Seeley WW, et al. Resting functional connectivity in the semantic appraisal network predicts accuracy of emotion identification. *NeuroImage Clin*. 2021;31:102755.
59. Benhamou E, Marshall CR, Russell LL, Hardy CJD, Bond RL, Sivasathiseelan H, et al. The neurophysiological architecture of semantic dementia: spectral dynamic causal modelling of a neurodegenerative proteinopathy. *Sci Rep*. 2020;10:16321.
60. Chiong W, Wilson SM, D'Esposito M, Kayser AS, Grossman SN, Poorzand P, et al. The salience network causally influences default mode network activity during moral reasoning. *Brain*. 2013;136:1929–41.
61. Hutchings R, Palermo R, Bruggemann J, Hodges JR, Piguot O, Kumfor F. Looking but not seeing: Increased eye fixations in behavioural-variant frontotemporal dementia. *Cortex*. 2018;103:71–81.
62. Rosen HJ, Allison SC, Schauer GF, Gorno-Tempini ML, Weiner MW, Miller BL. Neuroanatomical correlates of behavioural disorders in dementia. *Brain*. 2005;128:2612–25.
63. Eldaief MC, Brickhouse M, Katsumi Y, Rosen H, Carvalho N, Touroutoglou A, et al. Atrophy in behavioural variant frontotemporal dementia spans multiple large-scale prefrontal and temporal networks. *Brain*. 2023;146:4476–85.
64. Tao Y, Ficek B, Rapp B, Tsapkini K. Different patterns of functional network reorganization across the variants of primary progressive aphasia: a graph-theoretic analysis. *Neurobiol Aging*. 2020;96:184–96.
65. Brown JA, Deng J, Neuhaus J, Sibley IJ, Sias AC, Lee SE, et al. Patient-Tailored, Connectivity-Based Forecasts of Spreading Brain Atrophy. *Neuron*. 2019;104:856–68.e5.
66. Gordon E, Rohrer JD, Fox NC. Advances in neuroimaging in frontotemporal dementia. *J Neurochem*. 2016;138:193–210.
67. Bethlehem RAI, Paquola C, Seidlitz J, Ronan L, Bernhardt B, Consortium CC, et al. Dispersion of functional gradients across the adult lifespan. *NeuroImage*. 2020;222:117299.
68. Warren JD, Rohrer JD, Schott JM, Fox NC, Hardy J, Rossor MN. Molecular nexopathies: a new paradigm of neurodegenerative disease. *Trends Neurosci*. 2013;36:561–9.
69. Rohrer JD, Warren JD. Phenotypic signatures of genetic frontotemporal dementia. *Curr Opin Neurol*. 2011;24:542.

## ACKNOWLEDGEMENTS

We would like to thank all the participants from both the Paris and London sites for their dedication to research. The ECOCAPTURE study was funded by grant ANR-10-IAIHU-06 from the program "Investissements d'avenir", by grant FRM DEQ20150331725 from the foundation "Fondation pour la recherche médicale", and by the ENEDIS company: <https://www.enedis.fr/>. AB is funded by a PhD Fellowship from the Fondation Recherche Alzheimer and this work was started when supported by Fondation Vaincre Alzheimer. JDW receives grant support from the Alzheimer's Society, Alzheimer's Research UK, the Royal National Institute for Deaf People, the UCL/UCLH NIHR Biomedical Research Centre and the National Brain Appeal (Frontotemporal Dementia Research Studentship in Memory of David Blechner). JDR has received funding from a Miriam Marks Brain Research UK Senior Fellowship, an MRC Clinician Scientist Fellowship (MR/M008525/1) and the NIHR Rare Disease Translational Research Collaboration (BRC149/NS/MH) as well as the MRC UK

GENFI grant (MR/M023664/1), the Bluefield Project and the JPND GENFI-PROX grant (2019-02248). DSM received funding from the European Research Council (ERC) under the European Union's Horizon 2020 research and innovation programme (grant agreement No. 866533-CORTIGRAD), the Wellcome Trust Core Award and the NIHR Oxford BRC. RM is supported by France Alzheimer, Fondation Recherche Alzheimer, Fondation Philippe Chatrier and Rosita Gomez association.

## AUTHOR CONTRIBUTIONS

Conceptualisation: RM, AB, DSM; Data collection: LLR, BB, RL, JDW, JDR; Methodology: AB, VLD, DSM; Data analysis: AB, MH, DSM, RM; Manuscript writing: AB, DSM, RM; Manuscript reviewing: AB, VG, LLR, VLD, MH, ILB, BB, RL, JDW, JDR, DSM, RM.

## COMPETING INTERESTS

The authors declare no competing interests.

## ETHICS APPROVAL AND CONSENT TO PARTICIPATE

All methods were performed in accordance with the relevant guidelines and regulations. Each study was granted approval by the local ethics committee. The ECOCAPTURE study was approved by the "Comité de Protection des Personnes," on May 17, 2017 (CPP 17–31) and registered in a public clinical trial registry ([clinicaltrials.gov](http://clinicaltrials.gov): NCT03272230). The LIFTD study was granted approval by the London Queen Square Research Ethics Committee (ID 15/0805). All participants provided written informed consent prior to participating in the studies in accordance with the declaration of Helsinki. Anonymity was preserved for all participants.

## ADDITIONAL INFORMATION

**Supplementary information** The online version contains supplementary material available at <https://doi.org/10.1038/s41380-024-02847-4>.

**Correspondence** and requests for materials should be addressed to A. Bouzigues or R. Migliaccio.

**Reprints and permission information** is available at <http://www.nature.com/reprints>

**Publisher's note** Springer Nature remains neutral with regard to jurisdictional claims in published maps and institutional affiliations.



**Open Access** This article is licensed under a Creative Commons Attribution-NonCommercial-NoDerivatives 4.0 International License, which permits any non-commercial use, sharing, distribution and reproduction in any medium or format, as long as you give appropriate credit to the original author(s) and the source, provide a link to the Creative Commons licence, and indicate if you modified the licensed material. You do not have permission under this licence to share adapted material derived from this article or parts of it. The images or other third party material in this article are included in the article's Creative Commons licence, unless indicated otherwise in a credit line to the material. If material is not included in the article's Creative Commons licence and your intended use is not permitted by statutory regulation or exceeds the permitted use, you will need to obtain permission directly from the copyright holder. To view a copy of this licence, visit <http://creativecommons.org/licenses/by-nc-nd/4.0/>.

© The Author(s) 2024